Journal of Structural Geology, Vol. 3, No. 3, pp. 265 to 277, 1981.
Printed in Great Britain

0191-8141/81/030265-13 $02.00/0

Cleavage–fold relationships and their implications for transected folds: an example from southwest Virginia, U.S.A.

DAVID R. GRAY

Department of Geological Sciences, Virginia Polytechnic Institute and State University, Blacksburg, Virginia 24061 U.S.A.

(*Received* 12 *November* 1980; *accepted in revised form* 25 *June* 1981)

Abstract—A non-coaxial deformation involving pre-folding initiation of cleavage perpendicular to bedding is proposed to explain non-axial planar cleavage associated with mesoscopic folds in part of the Appalachian foreland thrust-belt of southwest Virginia. Folds are gently plunging, asymmetric, upright to slightly inclined, sinusoidal forms with non-axial fanning cleavage. They show extreme local variations in type and degree of transection and the consistency of transection direction. These relations are further complicated by hinge migration.

Cleavage–fan angles, bedding–cleavage angles and Δ transection values appear influenced by fold tightness, and in part by fold flattening strain. Fold flattening increments are considered simultaneous with folding. Axial surface traces, and not cleavage traces, coincide with the principal extension direction in fold profiles. Geometric modelling of cleavage fanning and bedding-cleavage angle variations for various theoretical folding modes suggest that folding in limestone and sandstone layers was by tangential longitudinal strain. Significant shape modification and change in bedding–cleavage relations occurred after limb dips of 40 and 50° were attained in limestone and sandstone respectively. Mud-rock class 1C folds with convergent cleavage fans show features transitional between buckling and flexural flow. Initiation of 'cleavage' fabrics during layer-parallel shortening prior to significant folding may be important for cleavage evolution in some deformed rocks.

INTRODUCTION

IMPLICIT in the earliest descriptions of cleavage in low-grade metamorphic rocks is a close geometrical and genetic relationship between cleavage and folding. The axial planar nature of cleavage to folds has long been recognised (see Sedgewick 1835, Darwin 1846, Rogers 1856). However, in recent years there has been increased awareness that cleavage does not have to develop precisely parallel to associated fold axial surfaces (e.g. Ramsay 1963, Moench 1970, Wickham 1972, Powell 1974, Stringer 1975, Borradaile 1978, 1979, Boulter 1979, Phillips *et al.* 1979, Stringer & Treagus, 1980). Transected folds (Powell 1974) with cleavage to axial-surface discordances greater than 45° have been recognized (see Powell 1974, Borradaile, 1978). Non-planar relationships have been attributed to the following mechanisms.

(1) Cleavage is initiated early in folding and remains coincident with the XY principal plane of strain (where $X > Y > Z$) during a non-coaxial deformation, whereas the fold axial surface rotates like a passive marker (Ramsay 1963).
(2) Cleavage develops synchronous or asynchronous with folding but only forms during part of a non-coaxial deformation sequence (Powell 1974, Stringer 1975). Asynchronous development has been related to high fluid pressure early in folding (Borradaile 1978, 1979).
(3) Cleavage develops synchronous with folding in layers oblique to directions of principal strain during either coaxial or non-coaxial deformation (Borradaile 1978, Stringer & Treagus 1980, Treagus 1981).
(4) Cleavage develops synchronous with folding in strike-slip zones of ductile - shear (Sanderson *et al.* 1980, fig. 8).

The timing of cleavage formation during folding has always been contentious (see Wood 1974, p. 369), but it is clear from the above hypotheses that this is an important aspect in establishing the cause of fold transection. Other aspects relate to the coaxiality of the deformation, the strain state, and whether cleavage and fold axial planes behave as passive markers or material surfaces during a progressive deformation. All these determine relationships between folds and their associated cleavage.

Geometrical relationships between cleavage and folds are used in this paper to investigate some transected mesoscopic folds in calcareous mudrocks (Ordovician Moccasin Formation) from the Valley and Ridge Province of south-west Virginia, U.S.A. (Fig. 1a). This portion of the Appalachian foreland zone is characterized by long, linear to arcurate, NE–SW trending thrust faults which truncate regional anticlines and synclines (Fig. 1a and b). The folds occur within the Narrows Thrust sheet and are minor structures on the south-east limb of the Clover Hollow anticline, a doubly plunging NE–SW trending regional fold. Relationships of these folds to the regional structure are presented elsewhere (Simon & Gray in review). The rocks are singly deformed and have undergone anchimetamorphism, with temperatures between 200 and 250°C based on conodont colour alteration (Epstein *et al.* 1976). The folds are exposed in roadcuts along Routes 601 and 604, approximately 1.6 km north of Newport, Virginia (Fig. 1c).

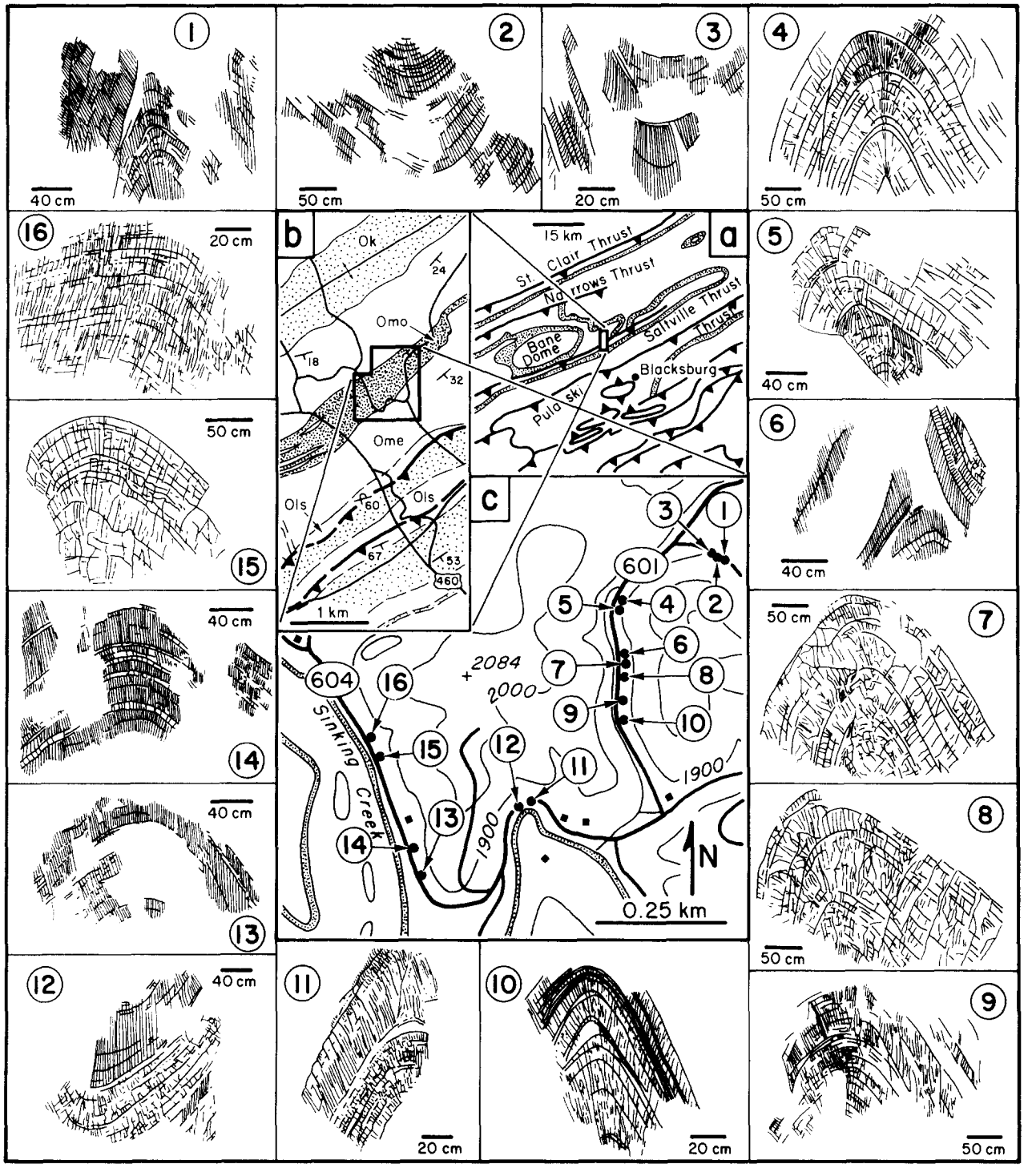

Fig. 1. Profile sketches and locations of folds in the Moccasin Formation, near Newport, Virginia, U.S.A. (a) Regional geological map showing outcrop traces of major thrust-faults in the northern part of the Southern Appalachians. The outcrop pattern of Middle Ordovician rocks is stippled. (b) Local geological map (OK: Knox Dolomite; Ols: Ordovician limestone; Omo: Moccasin Formation; Ome: Martinsburg Formation). (c) Outcrop map showing locations of sketched folds on County roads 601 and 604.

This paper documents the type, degree and consistency of fold transection. The relations between cleavage, fold axial surfaces and the direction of principal extension in fold profiles is used to investigate timing of cleavage development and folding. Geometric modelling of bedding–cleavage angle and cleavage fanning is used to determine modes of folding by comparison of observed and predicted values. Another explanation of transected folds is presented since cleavage–fold relations define a chronology which is largely inconsistent with previous hypotheses.

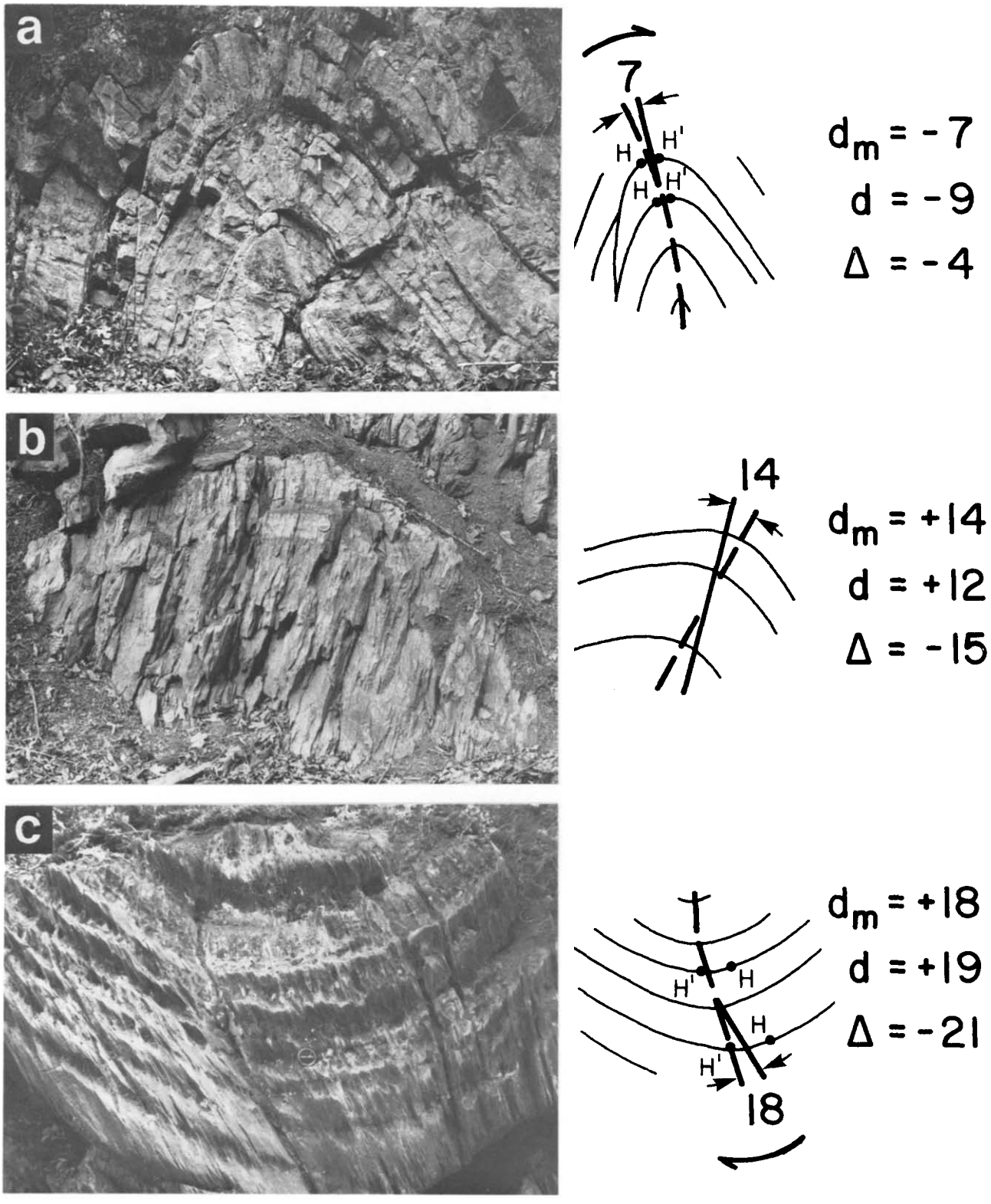

Fig. 2. Cleavage–fold relationships in profile views of folds. (a) Transected anticline in sandstone interbeds (fold 4, Fig. 1) showing a convergent cleavage fan. The fan angle is 80 to 90° and interlimb angle 50°. (b) Transected anticline in calcareous mudrock (fold 16, Fig. 1) showing weakly convergent cleavage fan. The fan angle is 17° and interlimb angle 114°. Cleavage is oblique to the axial plane by 14°. (c) Transected syncline in calcareous mudrock (fold 2, Fig. 1) showing a weakly convergent cleavage fan. The fan angle is 15° and interlimb angle 96°. Cleavages traces in the hinge deviate up to 18° from the axial surface trace.

H marks the position of the former hinge (where S_0 S_0 is 90°), and *H'* marks the present hinge (point of maximum bedding trace curvature). The solid half-arrow denotes the direction of hinge migration.

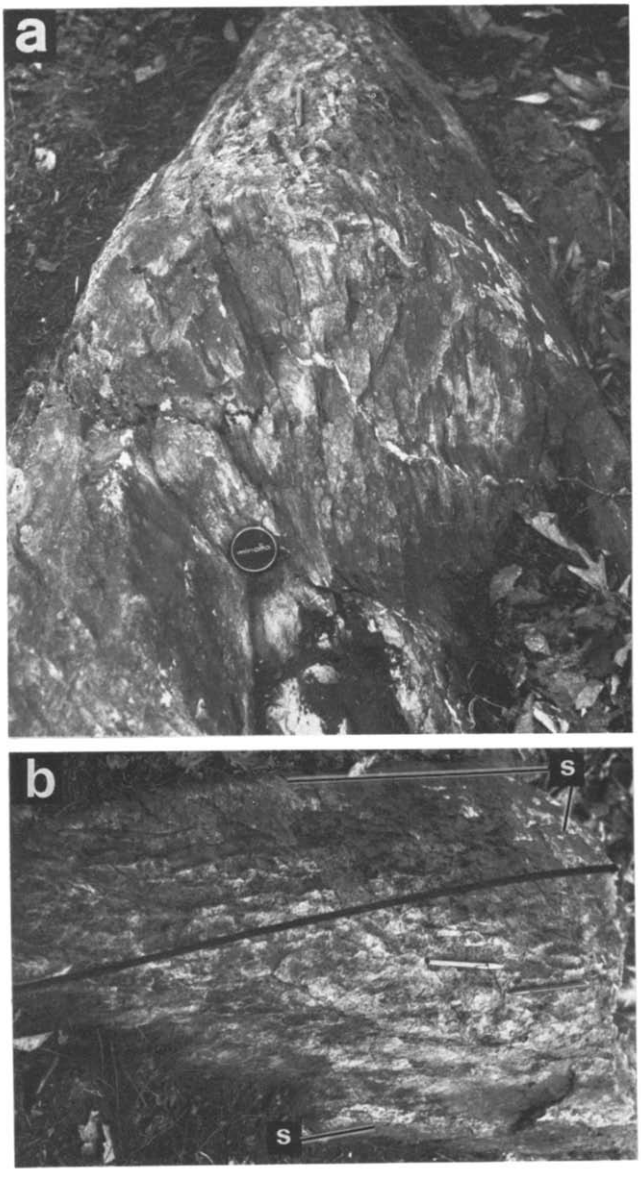

Fig. 3. (a) Transected fold in calcareous mudrock (fold 4, Fig. 1). The interlimb angle is 55° and cleavage fan angle 43°. Cleavage traces are not parallel to the axial-surface traces, d_m is +10° and d is +8°. (b) Hinge view of fold in (a) showing the bedding–cleavage intersection trace (black line) oblique to the fold hinge line (white pen). Δ is +7°. Fibrous calcite sheets labelled 's' occur along the bedding surface on the fold limbs.

MORPHOLOGY OF TRANSECTED FOLDS

Folds in the upper part of the Moccasin Formation are symmetric, upright to slightly inclined and gently plunging with approximately sinusoidal forms (Figs. 1 and 2). Geometry is alternating class 1B/1C and class 3 (Ramsay 1967), although some mudrock-layer folds are subsimilar with isogon inclinations approaching class 2. Amplitudes are up to 2 m and wavelengths range from 2 to 5 m. Interlimb angles range from 50 to 125° (50–90° in sandstone, 50–100° in limestone, 50–120° in mudrocks). Fold axial planes are oriented NE–SW, subparallel to the regional structural trend (Fig. 1b). Small contraction faults truncate the folds and have produced a complex sequence of anticlines ramped over anticlines. Synclines only occur where limestone and sandstone layers are present in their outer arcs.

Many of the folds contain calcite sheets along bedding partings (Fig. 3). These are generally not continuous across the folds but show sporadic development either on the limbs or around the hinges. They occur on bedding surfaces spaced at 30 cm to 1 m. Calcite in the sheets has fibrous habit with overlapping step-like structure typical of slickensides on fault surfaces. Crystal fibers are subparallel to bedding and are oriented at high angles to fold hinge-directions. Dilational structures also occur in some hinge zones (Fig. 1 :folds 2, 9, 10 and 11). These are open voids with saddle-reef form (see Ramsay 1974, fig. 12) but have no mineral infilling. Layer separations are up to 10 cm. Both features indicate that layer-parallel slippage has been important in fold development.

Local hinge migration is another feature of the folds. Curved (Fig. 2a) and bent (Fig. 2c) cleavage trajectories, and variable hinge displacements across fold profiles (Figs. 2a & c) suggest that hinge migration relates to differential interlayer movement either subsequent to or during cleavage development.

CLEAVAGE – FOLD RELATIONSHIPS

Spaced cleavages are intimately associated with the folds (Fig. 2). These range from a close spaced (40 μm spacing) domainal microfabric to a wider spaced (2–3 cm spacing), spaced disjunctive cleavage (see Gray in press). Both occur as non-axial cleavage fans (Figs. 2 and 3), for which the angular relationships are discussed below.

Fold transection

Cleavage locally transects mesoscopic folds (Figs. 3a & b). Two angles Δ and d (see Borradaile 1978, fig. 1) are needed to specify fold transection in three dimensions. Δ is the minimum angle between the cleavage plane and the fold axis, whereas d is the angle between the axial plane and the cleavage in the profile plane of the fold. These parameters define four end-member types of transected folds for a continuous spectrum of angular relationships (Fig. 4). Folds with truly axial plane cleavage have $\Delta = d = 0$, whereas transected folds with $d = 0$ show apparent axial plane-parallel cleavage in profile section. Folds with $\Delta = 0$ show cleavage–bedding intersection traces parallel to the fold hinge in hinge views. The graphed relationships (Fig. 4) can be used to specify the type of fold transection, the consistency of transection direction and the variation in degree of transection for a group of transected folds. For fanning cleavage, local cleavage orientation in the hinge is used as a reference for defining Δ and d.

Values of Δ and d from the folds investigated (see Appendix) have considerable variation; d values range from -6 to $+19°$ and Δ ranges from -21 to $+12°$ (Fig. 4). There is no consistent pattern in the transection of the folds by the cleavage. This may be due to (a) oblique superposition of cleavage on a set of folds with irregular hingelines; (b) synchronous development of cleavage and folds during a non-coaxial deformation and (c) folding of an early cleavage by either a set of regular or irregular folds during a non-coaxial deformation. The type of transection also varies through individual folds (see d_m values for folds 2, 4, 7, 12, 14 and 15 in the Appendix). The observed hinge migration (Fig. 2) during fold-shape modification by subsequent faulting, or flattening increments, will produce these variations. Cleavage is not superimposed on a regular set of folds, since transection relations would be consistent and (d, Δ) points would cluster to form a unimodal pattern in one of the quadrants. Relationships for cases (b) and (c) will vary depending on the degree of non-coaxiality of the deformation, and the degree of obliquity of the existing cleavage with the direction of folding for case (c). Distinction between (b) and (c) cannot be made using fold transection, although folded cleavage would result for case (c) if large discordances existed between cleavage and fold directions.

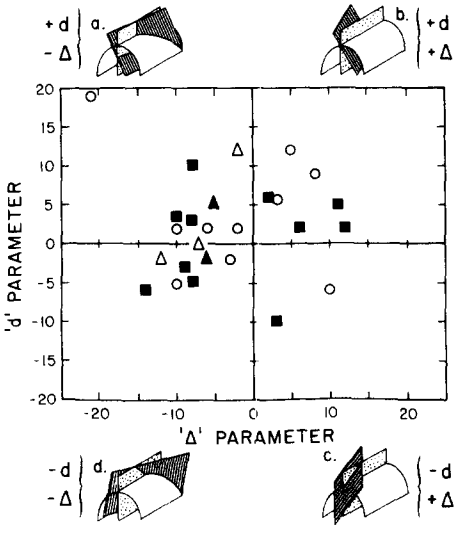

Fig. 4. (Δ, d) parameter graph. The diagrammatic sketches of folds illustrate the four end-member types of transected-folds (stippled plane, axial plane; lineated plane, cleavage). a + Δ indicates clockwise rotation of the cleavage towards the fold axis in hinge-view. a + d indicates clockwise rotation of the cleavage towards the axial plane in profile section. (see Borradaile (1978, fig. 1) for stereograph determination of Δ and d).

Cleavage fanning

Cleavage, as well as transecting mesoscopic folds, shows systematic fanning in profile-sections (Figs. 1 and 2). Both convergent and divergent cleavage fans are present. Convergent cleavage fans are common in class 1B/1C folds in limestone, sandstone and calcareous mudrock–argillaceous limestone, whereas divergent fans are associated with class 3 folds in calcareous mudrock. Convergent cleavage-fan angles (γ) range from 18 to 99°, with angles of 18–42° in calcareous mudrock, 66–99° in sandstone, and 62–83° in limestone (see Appendix).

The fan angle is also influenced by fold tightness (Fig. 5a). For sandstone and limestone, the fan angle decreases with increasing tightness, whereas for calcareous mudrock–argillaceous limestone it increases. The colinearity of data for the three lithologies suggests that each fold defines a point along a lithology-dependent deformation path (eg. heavy lines 1, 2 and 3, Fig. 5a) for the successive evolution of folds in terms of tightness and cleavage fan angle.

Although the axes of cleavage-fanning in the folds investigated do not correspond precisely with fold hinge-lines, fanning implies an intimate relationship between folding and cleavage development. Two interpretations of cleavage fanning exist:

(1) rotation of early formed cleavage during folding (Hills 1966, p. 306) with possible modification of bedding–cleavage angles during flattening increments and

(2) stress–strain refraction across mutilayer folds (see Dieterich 1969) with cleavage approximately tracking the XY plane of the local strain ellipsoid through individual layers during the deformation.

Both require cleavage development at least synchronous with folding. This implies that cleavage which developed late in folding should show little or no fanning.

Bedding–cleavage angle

The angle between bedding and cleavage ($S_0 \hat{} S_1$) varies systematically around folds. At inflection points of the measured folds $S_0 \hat{} S_1 = (\beta + \gamma)/2$ where β = interlimb angle and γ = cleavage fan angle: thus $S_0 \hat{} S_1$ is dependent on fold tightness and the type and degree of cleavage fanning. Distinct relationships exist for each lithology (Fig. 6a). Data from folds in particular lithologies are colinear suggesting once again that each fold defines a point on a progressive deformation path which represents successive stages in the evolution of fold shape and bedding–cleavage relationships.

In sandstone and limestone $S_0 \hat{} S_1$ remains at 90° until fold limb dips of 50 and 40° are attained respectively. The angles then change progressively to their finite state at a limb dip of 65° (see the heavy lines 2 and 3, Fig. 6a). $S_0 \hat{} S_1$ for calcareous mudrock–argillaceous limestone folds with convergent cleavage fans, decreases linearly to 42° for the lowest observed limb dip of 65° (see heavy line 1, Fig. 6a).

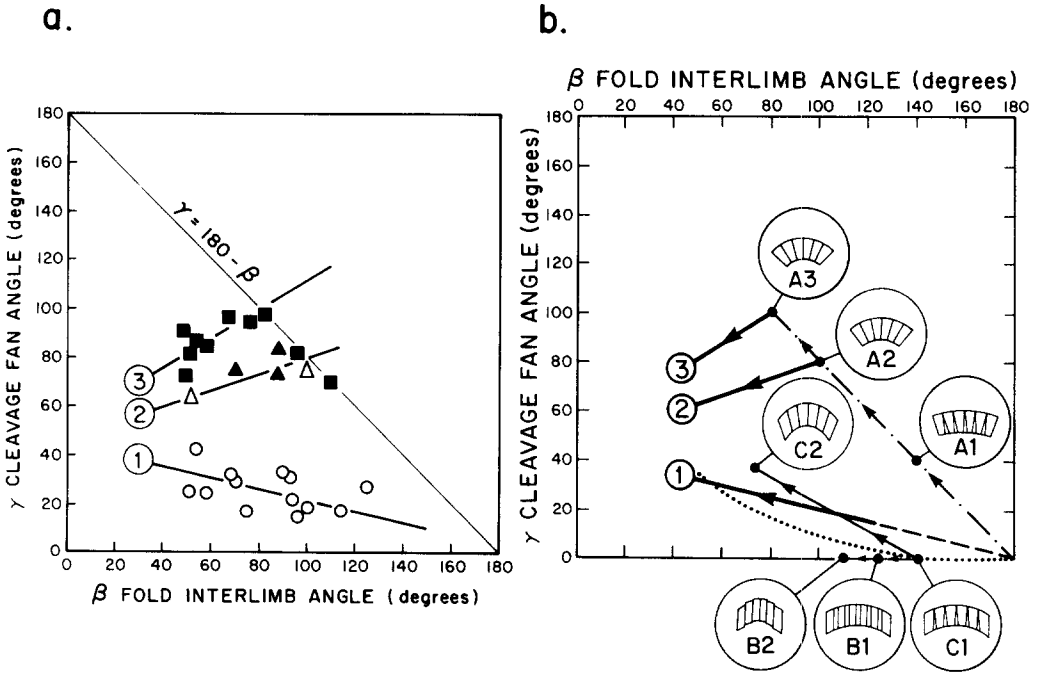

Fig. 5. Cleavage fan angle (γ) vs fold interlimb angle (β) graph. (a) Data plot for the investigated folds. 1, 2 and 3 represent best-fit lines for mudrock, limestone and sandstone respectively. (circle, calcareous mudrock; solid triangle, limestone; open triangle, thin interbeds of limestone and argillaceous limestone; solid square, sandstone). (b) Predicted γ and β relationships for specific modes of folding. Modes A, B and C correspond to the pressure-solution shape modification models of Groshong (1975, fig. 5). Mode A is also equivalent to buckling in tangential longitudinal strain. The dotted curve depicts relationships for flexural flow folding. Heavy lines 1, 2 and 3 indicate the observed γ and β relationships for mudrock, limestone and sandstone folds respectively.

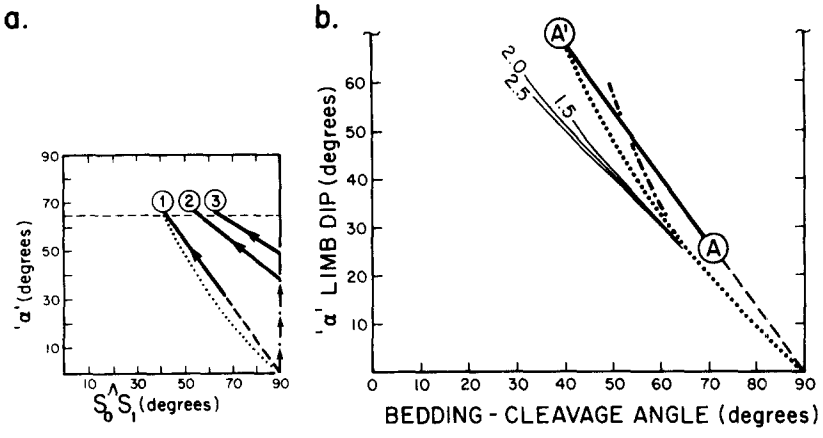

Fig. 6. Bedding cleavage angle (S^0S_1) vs limb dip (α) graphs. (a) Heavy lines 1, 2, 3 define the observed relationships for the mudrock, limestone and sandstone folds respectively. The dotted curve depicts relationships for a flexural-flow folding mode. (b) Enlargement of (a) showing predicted $S_0 \hat{} S_1$ relationships for flexural flow (dotted line), flattened flexural flow light solid lines with R_f values of 1.5, 2.0 and 2.5), and pressure-solution model C (dot-dash line). The heavy line A–A′ denotes the actual relationships for the mudrock folds.

FOLD FLATTENING ANALYSIS

The term 'flattening' is here used for shape modification of original parallel folds by finite homogeneous strain, following Ramsay (1967) and Hudleston (1973). It does not mean a flattening strain ellipsoid where $K < 1$. A modified t'_α analysis of class 1C folds is used, (Gray & Durney 1979, pp. 60–65) to determine the major axis X of the flattening strain in the fold profile.

The method uses the normal to cleavage traces in the fold hinge as the reference direction $\alpha = 0$ (Fig. 7a). Thickness measurements (t_α) are made at 5° intervals on both limbs of the fold and t'_α is calculated by normalising t_α against the maximum orthogonal thickness (t_{max}). A t'_α/α plot is then constructed for the fold half wavelength (Fig. 7b) and compared with the theoretical curves of Gray & Durney (1979 fig. 14) to derive the 'flattening' strain ratio R_f. The angle between the major axis of the fold flattening strain ellipse (X) and the trace of the hinge cleavage on the profile plane, is termed ϕ_s; the angle between X and the axial-surface trace is termed ϕ_A (Fig. 7b).

Values of ϕ_s, ϕ_A and R_f are given in the Appendix for the class 1C folds analysed. Log-polar double-angle graphs (Fig. 8) illustrate the relationships of angles ϕ_S ϕ_A with varied flattening. There is a 30° asymmetric scatter of X directions and their associated strain ratios (R_f) about the reference hinge cleavage with deviations from −10 to +20° (Fig. 8a). A 6° scatter is symmetrically distributed about reference axial plane traces with deviations from −3 to +3° (Fig. 8b).

Relationships between the flattening X directions, axial planes, and cleavages, for the folds investigated (Fig. 8) imply that cleavage is not superimposed on the folds during fold-flattening strain increments. If this were the

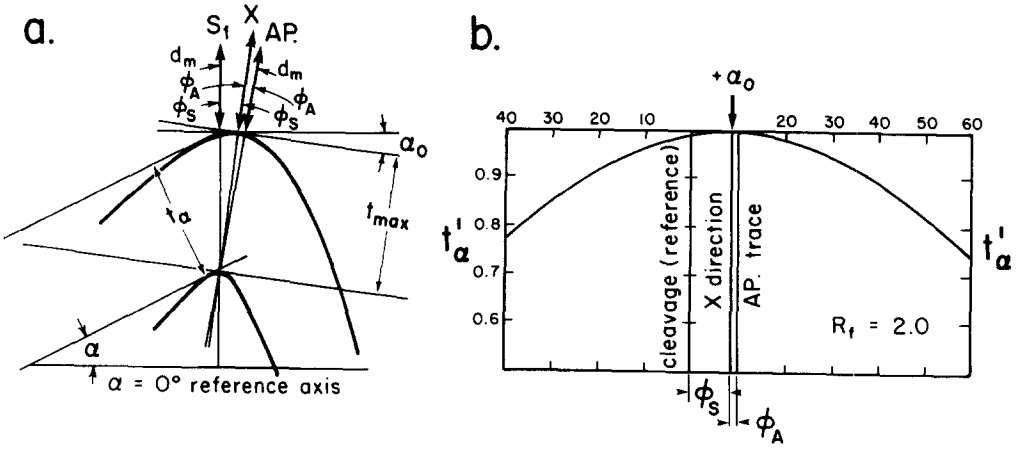

Fig. 7. Fold profile analysis, (a) Sketch of a fold in profile section with the cleavage trace (S_1), the fold axial plane trace (AP), the principal extension direction (X) in the fold profile, and designated angles ϕ_s, ϕ_A and d_m shown. + ϕ_s indicates a clockwise rotation of the axial surface towards the flattening direction. + d_m indicates a clockwise rotation of cleavage towatds the axial plane. (b) t'_α graph (see Gray & Durney 1979, fig. 14) showing a t'_α plot of the fold in (a) and the angles ϕ_s and ϕ_A. The cleavage trace was used as the reference direction (see text for discussion of method).

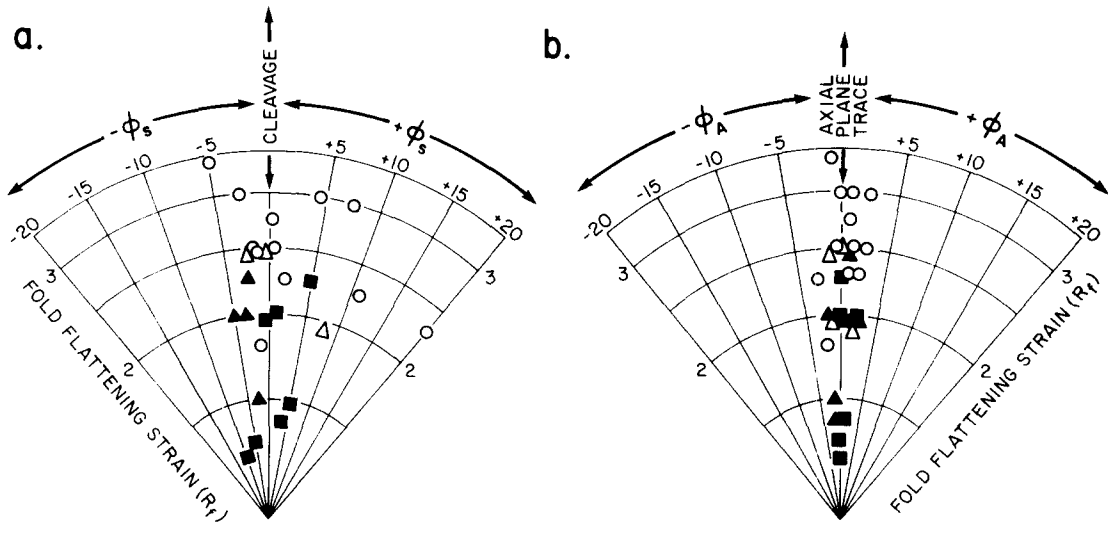

Fig. 8. Double-angle log-polar graphs showing fold-flattening strain ratios (R_f) plotted against cleavage as a reference in (a), and the axial plane trace as a reference in (b).

case, fold flattening directions would be grouped about the cleavage (see Gray & Durney 1979, fig. 12B). The significant scatter indicates that cleavage orientation is not directly relatable to fold flattening. The asymmetry in the distribution shows that cleavage in the folded layers was oblique to the principal directions of strain responsible for fold flattening. This requires modification of cleavage fabrics accompanied by rotation of cleavage surfaces clockwise towards the XY principal plane of fold flattening since most are at high angles to it (i.e. within 20°).

Oblique flattening of folds causes hinge migration along the folded layering (see Hudleston 1973, fig. 22). This requires the axial surface (AP) to approximately track the XY principal plane of fold flattening, particularly at high strains. Principal directions of extension (X) in fold profiles should therefore cluster about axial surface directions as shown by Fig. 8(b).

Timing of fold flattening

Since cleavage intensification and development is generally attributed to the propagation and decay stages of finite amplitude folding (Cobbold 1976), it is important to determine the timing of fold shape modification relative to folding. Shape modification simultaneous with folding will produce different cleavage–fold relations from those due to a superposed finite homogeneous strain.

Fold shape modification in the Moccasin Formation appears to have been simultaneous with buckling. There is no consistent variation, such as a regional gradient, in fold flattening. The flattening strain ratio (R_f), however, varies from fold to fold and is related to the tightness of individual folds (Fig. 9b). If fold flattening is simultaneous with buckling then the relationships in Fig. 8(a) require initiation of cleavage as a material surface prior to fold-shape modification (i.e. either prior to, or early in, folding). Cleavage orientation, and consequently the fan angle (γ), must therefore be influenced by fold flattening. Graphed relationships (Fig. 9a) show this for sandstone and limestone lithologies (see 2 and 3, Fig. 9a) but not for calcareous mudrock–argillaceous limestone. Similar relations are shown for the Δ transection parameter (Fig. 10a). Fold tightness appears to have a weak influence on Δ for sandstone and limestone, but not for mudrock. It is apparent that cleavage orientation in the latter is controlled by some other mechanism. The d transection parameter is independent of the interlimb angle (Fig. 10b).

IMPLICATIONS FROM THEORETICAL MODELS OF FOLD MECHANISMS

Folding mode and the associated shape-modification processes are categorized by characteristic patterns in terms of fold tightness, cleavage fanning and bedding–cleavage angles. Comparison of patterns from the measured folds (Figs. 5a and 6a) with those determined for theoretical models of folding (Figs. 5b and 6b) will therefore provide a direct method for defining the nature and interrelationships of folding and shape modification. Inferences can also be made about timing of cleavage development. It is stressed at this point that although the cleavages transect the folds, actual discordances in fold profiles for the folds investigated do not appear to significantly affect the modelling.

Convergent cleavage fan angles (γ) and bedding-cleavage angles ($S_0 \hat{} S_1$) have been calculated for various interlimb angles (β) and limb dips (α) respectively, for the folding modes of tangential longitudinal strain (cf. Ramsay 1967, fig. 7–63), flexural flow (cf. Ramsay 1967, fig. 7–54) and pressure-solution fold shape modification (cf.

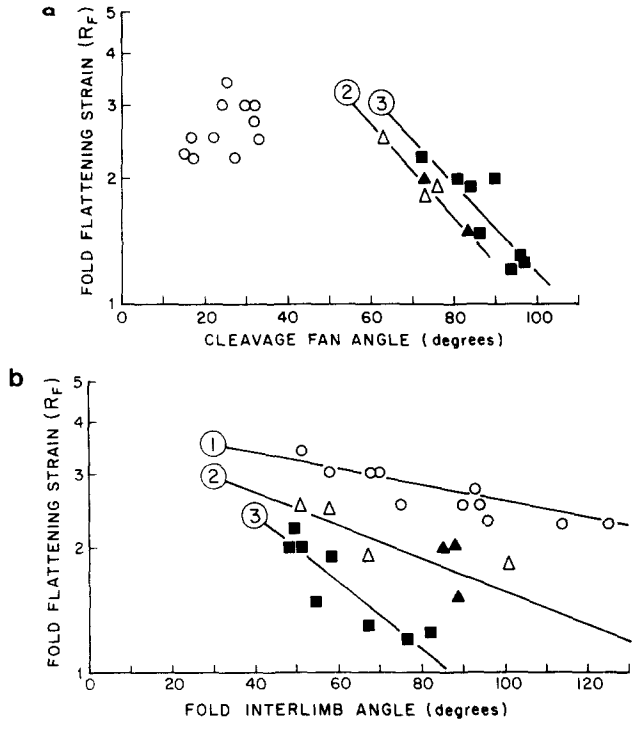

Fig. 9. Relationships between fold tightness, cleavage-fan angle and fold flattening strain ratio (R_f). (a) Cleavage fan angle (γ) vs flattening strain ratio (R_f) graph.
(b) Fold interlimb angle (β) vs flattening strain ratio (R_f) graph. (circle, calcareous mudrock; solid triangle, limestone; open triangle, thin interbeds of limestone and argillaceous limestone; solid square, sandstone). 1, 2, and 3 are the best-fit lines for mudrock, limestone and sandstone data respectively.

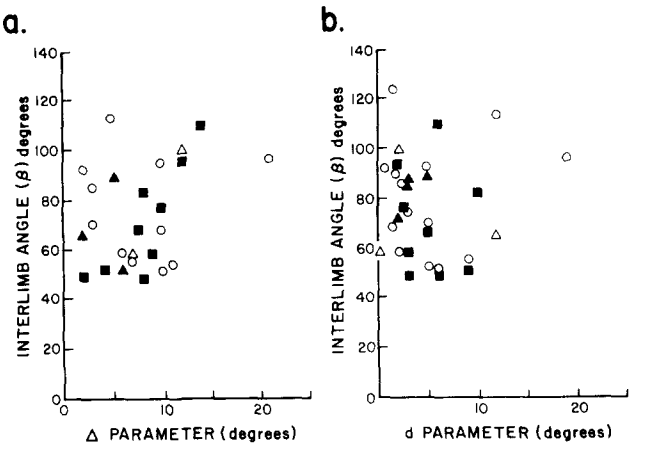

Fig. 10. Graphs of interlimb angle (β) vs the Δ transection parameter in (a), and the d transection parameter in (b).

Groshong 1975, fig. 5). The calculations were made assuming that 'cleavage' was (1) in existence prior to folding, (2) orthogonal to bedding prior to folding and (3) rotated as a material plane during folding. The validity of these assumptions will be discussed later.

Defined relationships between cleavage fan angle (γ) and fold interlimb angle (β) for the various fold modes are shown in Fig. 5b. Predicted relations between limb dip (α) and bedding–cleavage angle ($S_0 \hat{} S_1$) are plotted in Fig. 6(b). It is important to note that points along the heavy lines 1, 2 and 3, denoting relationships for the measured folds, represent successive stages in the evolution of the final fold shape. For a given limb dip, or interlimb angle, there is a specified bedding–cleavage angle and cleavage fan angle respectively, in each of the lithologies. This is in agreement with data from measured folds where cleavage fan angles, bedding–cleavage angles and Δ transection values appear influenced by fold tightness, and in part by fold flattening strain (R_f). Implications from the graphs (Figs. 5b and 6b) are that folds in limestone up to 40° limb dips have shapes, cleavage fans and bedding–cleavage angles equivalent to a tangential–longitudinal-strain model with layer-parallel-shortening strain ratios (R_i) in the range $1 \leq R_i \leq 1.6$. Folds in sandstone are equivalent to a tangential–longitudinal-strain model up to limb dips of 50° with strain ratios $1 \leq R_i \leq 1.4$.

Calcareous mudrock–argillaceous limestone folds show more complex cleavage–fold relationships, however. Trends indicate that these are not modified tangential–longitudinal-strain folds, not flexural flow folds *sensu stricto*, not flattened flexural-flow folds, and not pressure-solution model C modified folds *sensu stricto*. The heavy line A–A′ (Fig. 6b), representing the sequence of α vs $S_0 \hat{} S_1$ for the measured mudrock folds, lies close to but transects the calculated sequences for flexural flow and pressure-solution model C. The increase in fan angle with decreasing interlimb angle is clearly not a fold-flattening phenomenon (see also Fig. 9a), as this would cause γ to decrease rather than increase. It is suggested that calcareous mudrock–argillaceous limestone folds with convergent cleavage fans developed in a flexural-flow mode where an early-formed dominal microfabric (cf. Gray in press) approximated a non-material surface which tended to lag behind a line of passive marker points originally orthogonal to bedding. This would explain the observed discrepancy of the actual values from the calculated values. Further speculation from the graph is that although the early fabric lagged behind the orthogonal marker points for limb dips $0 \leq \alpha \leq 30$, between $30 \leq \alpha \leq 70$ this fabric material surface caught up with the passive marker points such that at $\alpha = 70$ the measured value coincided with those for flexural flow *sensu stricto*. This change perhaps relates to the development of the spaced disjunctive cleavage during the deformation sequence and implies an increase in the rate of pressure-solution around limb dips of 30° during folding. A change in the dominant deformation mode from controlled grain boundary sliding to pressure solution during a single, continuous deformation sequence is considered responsible (Gray in press).

The assumptions used in the comparative modelling involved cleavage orthogonal to bedding prior to folding and passive behaviour of cleavage during fold development. Since the observed relations at low limb dips closely match those predicted by the modelling for sandstone and limestone lithologies, their initial $S_0 \hat{} S_1$ is considered to be 90°. The initial $S_0 \hat{} S_1$ in calcareous

mudrock–argillaceous limestone may also have been close to 90° since data from open mudrock folds (Simon 1980, pers. comm.) shows that the extrapolation of line 1 (Fig. 6a) is correct. This requires cleavage initiation during an initial homogenous deformation (layer-parallel shortening; Milnes 1971) preceding significant folding. Similar relations have been recognized elsewhere (Nickelsen 1973, 1979, Geiser 1974, Ross & Barnes 1975, Beach 1977, Boulter 1979). Furthermore early penetrative strain, recorded by distorted fossils and development of spaced cleavages, has been documented for the weakly-deformed rocks at the leading edge of the Appalachian foreland fold zone (cf. Nickelsen 1966, Groshong 1975, Faill 1977, Engelder & Engelder 1977, Engelder & Geiser 1979).

The behaviour of the cleavage during the deformation has been more complex. Passive behaviour is only documented to this point for sandstone and limestone lithologies up to limb dips of 40 and 50° respectively. Non-passive behaviour, dependent on operative grain-scale deformation mechanisms, has been implied for calcareous mudrock–argillaceous limestone. The integrated modelling approach discussed below provides more information on cleavage behaviour.

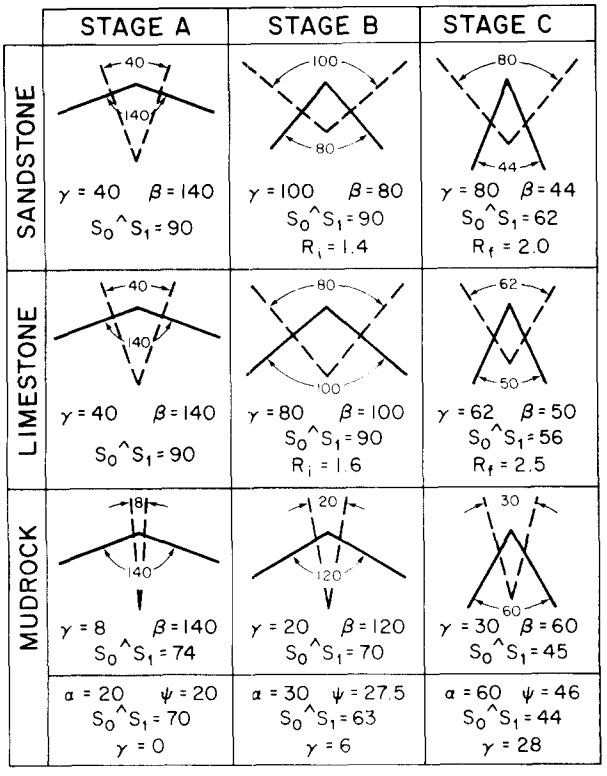

Fig. 11. Folding-simulation models illustrating cleavage–fold relations at three different development stages for sandstone, limestone and mudrock folds. Cleavage fan angle (γ), fold interlimb angle (β) and bedding-cleavage angles ($S_0 \hat{} S_1$) are given. (See text for discussion). Calculated $S_0 \hat{} S_1$ and γ values, assuming strictly flexural flow, are given for the mudrock at the base of the figure.

Integrated approach to modelling

Data on angular relations between bedding and cleavage were combined to produce two-dimensional representations of fold profiles for three different development stages of folds in sandstone, limestone and mudrock (Fig. 11). Previous modelling (Figs. 5b and 6b) treated each relationship separately. Symmetrical kink-forms were adopted for simplicity (cf. Boulter 1979).

For sandstone and limestone folds, *stage A* represents cleavage–bedding relationships in the transition from layer-parallel shortening to buckling. *Stage B* represents the transition from buckling to flattening, whereas *stage C* is the finite state. Stages *A*, *B* and *C* for the mudrock folds represent cleavage–folding relationships at three successive stages in the evolution of a mudrock fold. The modelling involves comparison of observed bedding–cleavage angles ($S_0 \hat{} S_1$) and cleavage fan angles (γ) with those predicted for given changes in fold interlimb angles for the transitions between the three fold stages.

Progress from stage *A* to *B* for both limestone and sandstone is characterized by passive rotation of bedding and cleavage during folding by tangential longitudinal strain such that $\gamma = 180 - \beta$ (see Fig. 5a). $S_0 \hat{} S_1$ remains at 90° but the folds develop an initial shape factor which give fold-flattening strain ratios (R_i) of 1.4 and 1.6 for sandstone and limestone respectively. Transition from stage *B* to *C* for standstone folds indicates an incremental fold flattening strain of 1.42 (R_S), since analysis of the initial and final fold shapes gives flattening strain ratios $R_i = 1.4$ and $R_f = 2.0$ and $R_i \times R_s = R_f$. Assuming passive S_1 behaviour, the strain (R_s) responsible for the change in S_1 orientation is also 1.42 since $\theta = 50°$ and $\theta' = 40°$ (see Ramsay 1967, eqn 3–34). The angles θ and θ' are between S_1 in this case, and the axial plane trace in profile-section (which in this analysis is assumed to be parallel to the X direction) before and after deformation respectively. However, angular relations of $\theta = 40°$ and $\theta' = 22°$ for bedding (S_0) indicate that the change in S_0 orientation was accompanied by limb rotation since the calculated R_s value of 2.1 is too high. Assuming R_s is 1.4, then a limb rotation of 7.5° occured in the sandstone. Similar relationships exist for the limestone. Since fold shapes give $R_i = 1.6$ and $R_f = 2.5$ then the strain (R_s) responsible for shape modification from stage *B* to *C* is 1.6. Angular relations of $\theta = 40°$ and $\theta' = 31°$ for S_1 implies an R_s of 1.4 for change in S_1 orientation. Values of $\theta = 50°$ and $\theta' = 25$ for S_0 give an R_s of 2.6. This value is similarly too high and indicates a limb rotation of approximately 12° in the limestone, accompanied fabric modification during flattening. The limb rotations in both lithologies are attributed to a modified flexural-slip mechanism where strain accommodation in the adjacent mudrock enables further rotation of competent-layer fold limbs. The analysis suggests therefore that cleavage in sandstone and limestone has largely behaved in a passive manner.

Previous investigation of the mudrock (Figs. 5b and 6b) has suggested bulk flexural-flow behaviour. Calculations of angular shear (ψ) due to flexural-flow (see Ramsay 1967, fig. 7–57) for the limb dips in the three fold stages (Fig. 11) give $S_0 \hat{} S_1$ values and cleavage fan angles (γ),

assuming cleavage rotated as a material plane originally perpendicular to bedding. $S_0 \hat{} S_1$ values approximately agree but observed cleavage–fan angles are markedly higher at low limb dips than predicted angles (Fig. 11). These differences may be related firstly to non-passive behaviour of the developing cleavage, and secondly to limb rotations concomitant with flexural-flow giving larger cleavage fan angles. The mudrock-layer folds selected for the investigation had class 1C geometry. These folds cannot result from flexural-flow *sensu-stricto*. The cleavage–fold relations and fold geometry show transitions between buckling and flexural-flow. Limb rotations are possible since the class 1C mudrock-layer folds generally occur adjacent to class 3 mudrock layer folds on their inner arcs.

DISCUSSION AND CONCLUSIONS

Prefolding initiation of cleavage is proposed for the Moccasin Formation of southwest Virginia. Development of cleavage non-axial planar to the folds could be due either to (1) closely related, successive, non-coaxial strains during a protracted progressive deformation or (2) a coaxial/non-coaxial deformation involving layers oblique to directions of principal strain (Borradaile 1978, Stringer & Treagus 1980, Treagus 1981). Other mechansims (see Introduction) are inconsistent with the fold, cleavage and strain orientation data.

Marked local variation in fold transection (Fig. 4) supports (1) since such irregularity would require either irregular orientated initial layering or markedly inhomogeneous strain if produced by model (2). Strains determined from reduction spots, in the mudrock where the folds were investigated (Simon & Gray in review), are relatively uniform and indicate no significant variation in local strain. These strains reflect deformation associated with protracted development of the domainal microfabric, probably up to fold–limb dips of 30°. The marked variations in fold flattening strain are related to position in the fold 'train' and to faults. A non-coaxial deformation history for these rocks is suggested by minor, but consistent shifts in cleavage, fold axes and fault planes (Simon 1981). Another explanation for transected folds is therefore proposed: non-coaxial deformation and folding of rocks with initial (pre-folding) bed–perpendicular cleavage. This may only be peculior to foreland zones composed of interleaved, stacked imbricate thrust-sheets, since early lateral shortening (up to 10–15%) is considered a necessary consequence of décollement tectonics (cf. Gwinn 1964, Engelder & Engelder 1977).

Investigation of angular relations between cleavage, fold axial surfaces, and bedding may provide useful information on the timing of cleavage development with respect to folding. Observed cleavage fanning, bedding–cleavage angle, and fold tightness relations can be compared with those predicted from theoretical modes of folding. This is potentially an objective discriminator for determining mechanisms of folding in naturally deformed rocks. Application of this approach to folded sandstone, limestone and mudrock of the Moccasin Formation of southwest Virginia has shown that:

(1) Folds in limestone and sandstone developed by buckling in a tangential–longitudinal-strain mode up to limb dips of 40 and 50° respectively, but were modified by flattening increments in the decay stage to produce the final fold shape and bedding–cleavage relationships. Cleavage essentially behaved in a passive manner.

(2) Folds in calcareous mudrock argillaceous limestone (class 1C geometry) developed largely in a flexural-flow mode. Cleavage did not behave as a passive marker, since predicted bedding–cleavage angles ($S_0 \hat{} S_1$) for flexural-flow are significantly lower than the observed angles.

(3) Changes in bedding–cleavage angle due to angular shear and/or fold flattening cannot produce the observed values of limb dip for all lithologies. This requires limb rotation due to strain accommodation in adjacent class 3 mudrock layer folds.

Migration of fold hinges is probably an important part of fold amplification and propagation, particularly those which develop asymmetry. In the Moccasin Formation hinge migration appears related to differential inter-layer slippage during bulk modification of fold shape by fold flattening and/or contraction faulting.

Acknowledgements—I thank anonymous reviewers for critical comments which improved the manuscript. Support for the research was provided by National Science Foundation Grant No. EAR 79-19703 and by a VPI & SU College of Arts and Sciences Small Projects Grant in the initial stages. I am grateful to Robert Simon for access to unpublished data and for discussion during the course of the work, and to S. W. Mauney for help in initial data collection. Drafting, photography and typing assistance was provided by VPI & SU and the respective services of Martin Eiss, Cynthia Zauner and Donna Williams are gratefully acknowledged. Finally I am indebted to Dr. W. D. Lowry for stimulating my interest in Valley and Ridge structural geology.

REFERENCES

Beach, A. 1977. Vein arrays, hydraulic fractures and pressure-solution structures in a deformed flysch sequence, S. W. England. *Tectonophysics* **40**, 201–225.

Borradaile, G. J. 1978. Transected folds: A study illustrated with examples from Canada and Scotland. *Bull. geol. Soc. Am.* **89**, 481–493.

Borradaile, G. J. 1979. Strain study of the Caledonides in the Islay region, SW Scotland: implications for strain histories and deformation mechanisms in greenshcists. *J. geol. Soc. Lond.* **136**, 77–88.

Boulter, C. A. 1979. On the production of two inclined cleavages during a single folding event; Stirling Range, S.W. Austrailia. *J. Struct. Geol.* **1**, 207–219.

Cobbold, P. R. 1976. Fold shapes as functions of progressive strain. *Phil. Trans. R. Soc.* **A283**, 129–139.

Darwin, C. 1846. *Geological Observations in South America*. Smith-Elder, London.

Dieterich, J. H. 1969. Origin of cleavage in folded rocks. *Am. J. Sci.* **267**, 155–165.

Engelder, T. & Engelder, R. 1977. Fossil distortion and décollement tectonics on the Appalachian Plateau. *Geology* **5**, 457–460.

Engelder, T. & Geiser, P. A. 1979. The relationship between pencil cleavage and lateral shortening within the Devonian section of the Appalachian Plateau, New York. *Geology* **7**, 460–464.

Epstein, A. G., Epstein, J. B. & Harris, L. D. 1976. Conodont colour alteration—an index to organic metamorphism. *Prof. Pap. U.S. geol. Surv.* **995**, 1–27.

Faill, R. T. 1977. Fossil distortion, Valley and Ridge Province, Pennsylvania. *Bull. geol. Soc. Am.* **9,** 262–263.

Geiser, P. A. 1974. Cleavage in some sedimentary rocks of the Central Valley and Ridge Province, Maryland. *Bull. geol. Soc. Am. 85,* 1399–1412.

Gray, D. R. in press. Compound tectonic fabrics in singly folded rocks from southwest Virginia, U.S.A. *Tectonophysics* (Aug, 1981).

Gray, D. R. & Durney, D. W. 1979. Investigations of the mechanical significance of crenulation cleavage. *Tectonophysics* **58,** 35–79.

Groshong, R. H. 1975. Slip cleavage caused by pressure solution in a buckle fold. *Geology* **3,** 411–413.

Gwinn, V. E. 1964. Thin-skinned tectonics in the plateau and the northwestern Valley and Ridge provinces of the Central Appalachians. *Bull. geol. Soc. Am.* **75,** 863–900.

Hills, E. S. 1966. *Elements of Structural Geology.* Chapman & Hall, London.

Hudleston, P. J. 1973. Fold morphology and some geometrical implications of theories of fold development. *Tectonophysics* **16,** 1–46.

Moench, R. H. 1970. Premetamorphic down-to-basin faulting, folding, and tectonic dewatering, Rangeley area, western Maine. *Bull. geol. Soc. Am.* **81,** 1463–1496.

Milnes, A. G. 1971. A model for analyzing the strain history of folded competent layers in deeper parts of orogenic belts. *Eclog. geol. Helv.* **64,** 335–342.

Nickelsen, R. P. 1966. Fossil distortion and penetrative rock deformation in the Appalachian plateau, Pennsylvania. *J. Geol.* **74,** 924–931.

Nickelsen, R. P. 1973. Deformation structures in the Bloomsburg Formation. In: *Structure and Silurian and Devonian Stratigraphy of the Valley* and *Ridge Province in Central Pennsylvania* (edited by Faill, R. T.) Pennsylvania Bur. Topographic and Geologic Survey, Dept. of Environmental Resources, 119–129.

Nickelsen, R. P. 1979. Sequence of structural stages of the Allegheny Orogeny, at the Bear Valley Strip Mine, Shamokin, Pennsylvania. *Am. J. Sci.* **279,** 225–271.

Phillips, W. W. A., Flegg, A. M. & Anderson, T. B. 1979. Strain adjacent to the Iapetus Suture in Ireland. In: *The Caledonides of the British Isles—Reviewed* (edited by Harris, A. L., Holland, C. H. & Leake, B. E.) *Spec. Publ. geol. Soc. Lond.* 8.

Powell, C. McA. 1974. Timing of slaty cleavage during folding of Precambrian rocks, northwest Tasmania. *Bull. Geol. Soc. Am.* **85,** 1043–1060.

Ramsay, J. G. 1963. Structural investigations in the Barberton Mountain Land, eastern Transvaal. *Trans. Proc. geol. Soc. S. Afr.* **66,** 353–401.

Ramsay, J. G. 1967. *Folding and Fracturing of Rocks.* McGraw Hill, New York.

Rogers, H. D. 1856. On the laws of structure of the more disturbed zones of the earth's crust. *Trans R. Soc. Edinb.* **21,** 431–472.

Sedgewick, A. 1835. Remarks on the structure of large mineral masses, and especially on the chemical changes produced in aggregation of stratified rocks during different periods after their depostion. *Trans. geol. Soc. Lond. Ser.* 2, **3,** 461–486.

Sanderson, D. J., Andrews, J. R., Phillips, W. E. A. & Hutton, D. H. W. 1980. Deformation studies in the Irish Caledonides. *J. geol. Soc. Lond.* **137,** 289–302.

Simon, R. I. 1981. Mesoscopic structure and strain in part of the Narrows Thrust-sheet, Giles County, Virginia. Unpublished M.Sc. Thesis, Virginia Polytechnic Institute and State University.

Simon, R. I. & Gray, D. R. in review. Implications of strain and mesoscopic structure in part of the Narrows Thrust-sheet of the southern Appalachian foreland zone. *J. Struct. Geol.*

Stringer, P. 1975. Acadian slaty cleavage noncoplanar with fold axial surfaces in the northern Appalachians. *Can. J. Earth. Sci.* **12,** 949–961.

Stringer, P. & Treagus, J. E. 1980. Non-axial planar S_1 cleavage in the Hawick Rocks of the Galloway area, Southern Uplands, Scotland. *J. Struct. Geol.* **2,** 317–331.

Treagus, S. H. 1981. A theory of stress and strain variations in viscous layers, and its geological implications. *Tectonophysics* **72,** 75–103.

Wickham, J. S. 1972. Structural history of a portion of the Blue Ridge, northern Virginia. *Bull. geol. Soc. Am.* **83,** 723–760.

Wood, D. S. 1974. Current views of the development of slaty cleavage. *Rev. Earth Planet. Sci.* **2,** 369–401.

APPENDIX

Table of fold data (see text for details)

Fold Nos	layer	β	γ	R_f	ϕ_s	ϕ_A	d_m	d	Δ	Fold type	Rock type
1	A	75	17	2.5*	−2	+1	−3	—	—	A	mudrock
	B	52	63	2.5*	−2.5	0	−2	−2	−6	A	limestone
	C	52	7	—	—	—	—	—	—	—	mudrock
2	A	96	15	2.3	+20	+2	+18	+19	−21	S	mudrock
	B	88	73	2.0	+5	+2	+3	—	—	S	limestone
	C	85	78	2.0	−3	+1	−3	—	—	S	limestone
3	A	70	30	3.0	+7.5	+2.5	+5	+6	+3	S	mudrock
4	A	51	81	2.0*	−5	+2	−7	−9	−4	A	sandstone
	B	48	90	2.0	+1	0	+1	+3	−8	A	sandstone
	C	55	43	—	—	—	+10	+9	+7	A	mudrock
5	A	67	96	1.3	−5	−1	−4	−5	−8	A	sandstone
	B	85	20	—	—	—	−2	−2	−3	A	mudrock
6	A	49	72	2.25	+5	0	+5	+6	+2	A	sandstone
	B	54	86	1.49	+5.5	+0.5	+5	+5	+11	A	
7	A	82	97	1.25	−10.5	−0.5	−10	—	—	A	sandstone
	B	95	80	—	—	—	+3	+2	+12	A	sandstone
	C	82	97	—	—	—	+9	+10	−8	A	sandstone
8	A	51	25	3.4	−5	−1	−4	−6	+10	A	mudrock
	B	93	31	2.75	+0.25	+0.75	−0.5	—	—	A	mudrock
9	A	90	33	2.5	+1	−0.5	+1.5	+2	−2	A	mudrock
	B	88	84	1.5	+2.75	−1.25	+4	+5	−5	A	limestone
10	A	65	75*	1.9	+8.5	−1.5	+9.5	+12	−2	A	interbeds
	B	68	32	3.0	+2.75	+0.25	+2.5	+2	−10	A	mudrock
11	A	58	94*	2.49	−0.75	−1.75	+1	0	−7	A	interbeds
12	A	58	24	3.0*	−4.5	+1	+3.5	+2	−6	S	mudrock
	B	58	84	1.9	−0.5	+0.5	−1	−3	−9	S	sandstone
13	A	94	22	2.5	−1.5	+2.5	−4.5	−5	−10	A	mudrock
14	A	125	27	2.25	+2	+0.5	+1.5	—	—	A	mudrocks
	B	100	74*	1.8	−0.5	+1.5	−2	−2	−12	A	interbeds
15	A	110	68	—	—	—	−5	−6	−14	A	sandstone
	B	76	94	1.4	+3.5	+0.5	+3	+3	−10	A	sandstone
16	A	114	17	2.25	+11	−3	+14	+12	+5	A	mudrock

Key

β, interlimb angle (degrees);;
γ, cleavage fan angle (degrees),
R_f, fold flattening strain;
ϕ_s, angular deviation of cleavage trace (S_1) with R_f direction in fold profile plane (degrees);
ϕ_A, angular deviation of axial plane trace (AP) with R_f direction in fold profile plane (degree);
d_m, measured deviation of cleavage trace (S_1) with axial plane trace (AP) in fold profile plane (measured off photographs) (degrees);
d, angle between cleavage and axial plane in fold profile plane (determined off stereogram) (degrees);
Δ, dihedral angle between the cleavage plane and the fold axis (determined off Fold type, (A = anticline, S = syncline).